Supporting Information for
"Universal Mechanism of Bandgap Engineering in Transition-Metal Dichalcogenides"

Mingu Kang,[†] Beomyoung Kim,[†,‡] Sae Hee Ryu,[†] Sung Won Jung,[†] Jimin Kim,[†]

Luca Moreschini,[†,‡] Chris Jozwiak,[‡] Eli Rotenberg,[‡] Aaron Bostwick,[‡] and Keun Su Kim*,[†]

[†]Department of Physics, Pohang University of Science and Technology, Pohang 37673, Korea

[‡]Advanced Light Source, E. O. Lawrence Berkeley National Laboratory, Berkeley, CA 94720, USA

*E-mail: keunsukim@postech.edu. Phone: +82-10-3352-0158.

Contents

1. **Supporting Figures**

2. **Supporting Table**

3. **Screening Length of Space Charge Layers**
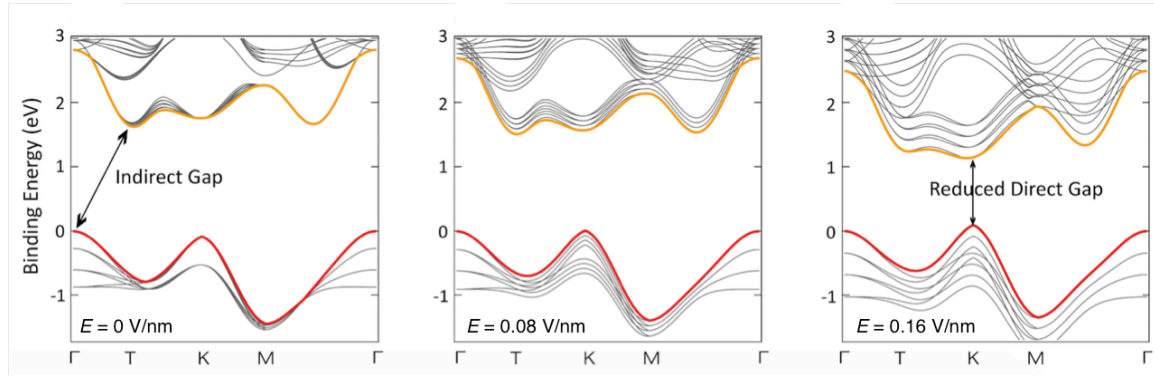
1. Supporting Figures

Figure S1. A series of tight-binding band calculation for four-layer 2H-TMDs with the vertical electric field, as marked at the bottom left of each panel. Double-head arrows indicate the indirect-to-direct bandgap transition. The results show essentially the same behaviors as those for bilayer 2H-TMDs (Figure 1d−f).
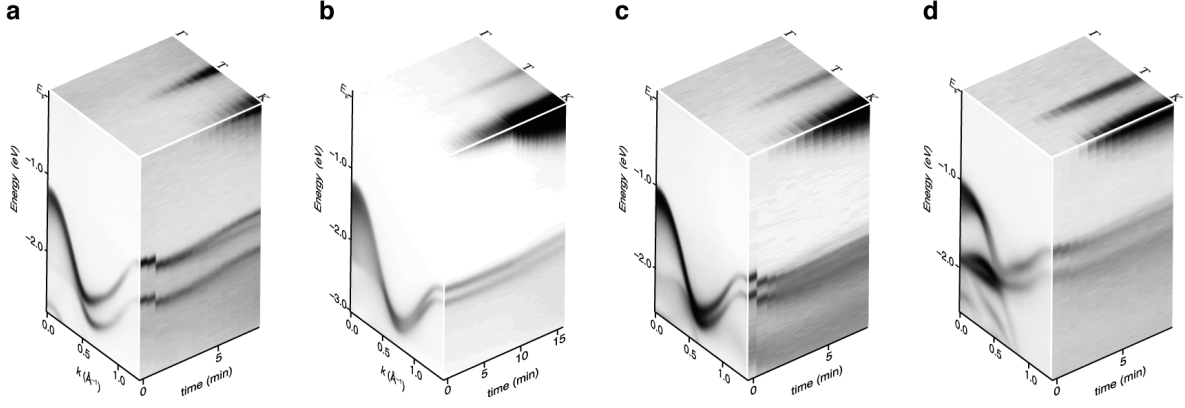
a **b** **c** **d**

Figure S2. Continuous doping series of ARPES spectra. (a)−(d), 3D representations of ARPES spectra taken with fine doping steps for WSe_2 (a), MoS_2 (b), $MoSe_2$ (c), and $MoTe_2$ (d) (see Figure 3a for WS_2). The key aspects of our observations in WS_2, bandgap modulations and VB splitting, are consistently observed in a−d.
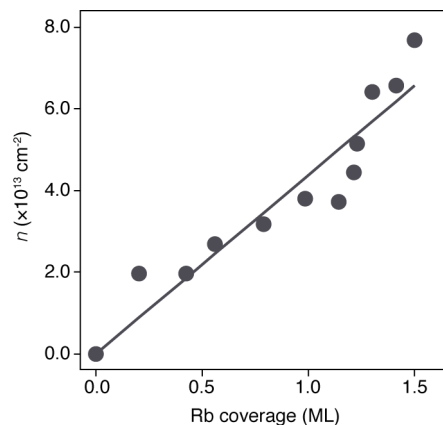
Figure S3. Monotonic charge transfer from dopants. Electron concentration n plotted as a function of the Rb coverage in units of ML. The coverage of 1.5 ML is determined on the basis of characteristic Rb $4p$ core-level spectra.[33] The intermediate coverage was then extrapolated from the areal ratio of Rb $4p$ core-level spectra after subtracting the background (that of pristine 2H-TMDs). The relation between n and the Rb coverage is approximately linear (overlaid line), indicating the monotonic charge transfer from Rb atoms to the surface 2H-TMDs layers.
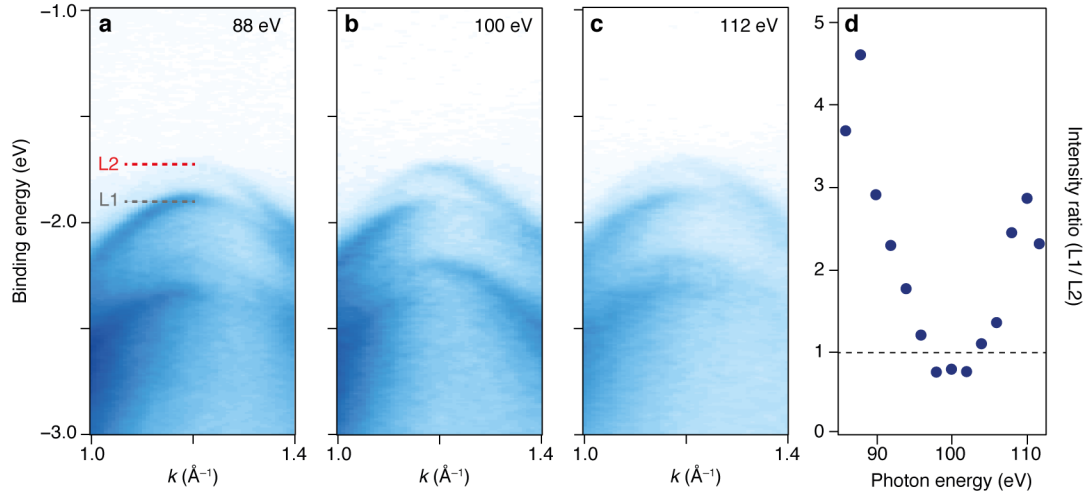
Figure S4. Layer origin of split valence bands. (a)−(c) Magnified ARPES data of WS$_2$ near the K point after the deposition of Rb, taken with different photon energies marked at the upper left. The split valence bands are denoted as L1 and L2 in a, corresponding to their layer origin, as discussed in the text. (d) The intensity ratio of L1 to L2 as a function of the photon energy. The ARPES intensity of L1, averaged over finite k (± 0.05 Å^{-1} with respect to the K point), is always greater than that of L2 over the photon energy that covers more than a Brillouin zone. This can be explained by the finite escape depth, which indicates that L1 and L2 originate from upper and lower layers, respectively, in the surface bilayer of 2H-TMDs.

2. Supporting Table

Table S1. Band parameters for 2*H*-TMDs. The lattice constants of 2*H*-TMDs (*c*/*a*) are obtained from the previous report.[8] The valence band splitting at the K point is directly measured from our ARPES spectra in Figure 2a,e,i,m,q. The Stark constant, defined by bandgap reduction per Rb coverage, and spin splitting per Rb coverage were obtained from a series of our ARPES spectra in Figure 2. The effective mass of conduction bands at K and T points is determined by fitting band dispersions with a parabolic function.

	Pristine TMDs			Doped TMDs			
	c/*a*	Bandgap at K (eV)	VB splitting at K (eV)	Stark constant (eV/ML)	Spin splitting (eV/ML)	Effective mass of CB at T (m_e)	Effective mass of CB at K (m_e)
WS₂	3.908	1.95	0.460	0.202	0.087	0.435	0.231
MoS₂	3.891	1.90	0.197	0.196	0.070	N/A	0.100
WSe₂	3.949	1.55	0.495	0.277	0.125	0.333	0.194
MoSe₂	3.922	1.58	0.201	0.460	0.193	N/A	0.168
MoTe₂	3.966	1.20	0.282	0.276	0.089	N/A	0.236

3. Screening Length of Space Charge Layers

Under thermal equilibrium, the number of electrons (n_c) and holes (p_v) in semiconductors can be described by

$$n_c(T) = \int_{E_c}^{\infty} g_c(E) \frac{1}{e^{(E-\mu)/k_BT}+1} dE \tag{1}$$

$$p_v(T) = \int_{-\infty}^{E_v} g_v(E) \frac{1}{e^{(\mu-E)/k_BT}+1} dE \tag{2}$$

where g_c and g_v are the density of states in conduction and valance bands, respectively, μ is the chemical potential, and k_B is the Boltzman constant.

In nondegenerate semiconductors with the quadratic approximation, the above expression can be rewritten as follows

$$n_c(T) = \frac{1}{4}(\frac{2m_c k_B T}{\pi\hbar^2})^{3/2} e^{-(E_c-\mu)/k_BT} \tag{3}$$

$$p_v(T) = \frac{1}{4}(\frac{2m_v k_B T}{\pi\hbar^2})^{3/2} e^{-(\mu-E_v)/k_BT} \tag{4}$$

where m_c and m_v are the effective mass of conduction and valance bands, and $\hbar$ is the reduced Planck constant.

We found from Figure 2a that the E_F of our pristine WS$_2$ is well above the charge neutrality point, indicating that the sample is n-doped. The screening effect is mainly governed by electrons in the conduction band whose density can be estimated as n_c = 2.67×10^{13} cm^{-3} with $m_c = 0.435 m_e$ cm^{-3}, $E_c - \mu = 0.083$ eV, and $T = 90$ K.

The length of space charge layers can be estimated based on the Thomas-Fermi screening theory. The Thomas Fermi wavevector k_0 is given by

$$k_0^2 = 4\pi e^2 \frac{\varepsilon_0}{\varepsilon} \frac{\partial n}{\partial \mu} = 4\pi e^2 \frac{\varepsilon_0}{\varepsilon} \frac{n}{k_BT} \tag{5}$$

where ε_0 and ε are the dielectric constant of vacuum and 2H-TMDs, respectively. With n_c = 2.67×10^{13} cm^{-3}, we found the screening length (inverse k_0) about 280 nm. This sizable length of space change layers supports the validity of the Thomas-Fermi screening theory.